



Design and experimental research of magnetically excited rotating piezoelectric energy harvester

Lipeng He¹ · Zhe Wang¹ · Gang Yu¹ · Ziyu Shen¹ · Shuai Jiang¹ · Guangming Cheng²

Received: 14 January 2021 / Accepted: 22 March 2022 / Published online: 17 May 2022
© The Author(s), under exclusive licence to Springer-Verlag GmbH Germany, part of Springer Nature 2022

Abstract

Piezoelectric energy harvesting is a widely used and environmentally friendly power generation technology, which can provide power for wireless electronic devices and low-power sensors. In this paper, a magnetically excited rotating piezoelectric energy harvester is proposed, which can generate output voltages of more than 15 V at frequencies below 13 Hz, where the maximum output voltage is 55.62 V. Through the rotation of the rotamer, magnetic coupling between magnetic blocks drives piezoelectric elements to vibrate nonlinearly to generate electrical energy. Structural prototypes with different parameters were designed and produced after analyzing the working principle and theoretical model of the entire piezoelectric system, and a series of experimental verifications were carried out on the theoretical model. The experimental results show that the energy harvester has the best power generation effect when the weight of the magnet mass is 6 g, the radial excitation distance is 5 mm, and multiple piezoelectric beams are connected in series. When the piezoelectric beams are connected in series and rotational speed is 550 r/min, the external load resistance is 75 k Ω , its maximum root mean square output voltage and average output power are 33.12 V and 14.625 mW, respectively. The energy harvesting system can light up 260 LED lights under the excitation of 550 r/min.

Keywords Piezoelectric · Energy harvester · Nonlinear · Magnetic field · Rotational

1 Introduction

Portable electronic devices, and wireless sensor networks have been developed rapidly in recent years, and gradually apply to municipal, military, medical and industrial production and other fields. Traditional batteries have problems such as low energy density, the need for periodic replacement or charging, and environmental pollution, and it is difficult to meet the needs of the rapid development of microelectronic products. Collecting vibration energy from the surrounding environment can solve these tedious battery replacement problems (Makki and Pop-Iliev 2012; Kamenar

et al. 2015). Achieving this goal depends on the progress of energy harvesting technology, which converts useless vibration energy in the environment into useful electrical energy to power certain microelectronic devices (Li et al. 2017; Deng et al. 2018). Piezoelectric energy harvesters (PEH) have received widespread attention due to their large output energy density, simple structure, and ease of processing, as well as miniaturization and integrated comfort.

The most PEHs are used as linear vibration resonators, where system performance is largely dependent on the resonance frequency. Conventional PEH consists of single or double cantilever beams with quality assurance at the free end. It is a typical linear resonator and has good performance in a narrow bandwidth (Binyet et al. 2018; Mangaiyarkarasi et al. 2019), and operates at the first resonance frequency. When the internal natural frequency of the system is consistent with the excitation frequency, it has the best power generation performance. Once the two frequencies do not match, the power generation performance will drop rapidly. To develop systems with broadband energy harvesting capabilities, many types of research have been done.

✉ Lipeng He
lipeng_he@126.com

✉ Zhe Wang
zhewang0926@163.com

¹ School of Mechatronic Engineering, Changchun University of Technology, Changchun, Jilin, China

² Institute of Precision Machinery, Zhejiang Normal University, Jinhua, China

Adjusting the resonance frequency of PEH provides an opportunity to improve the efficiency of power generation (Halim and Park 2017; Somkuwar et al. 2018). Automatically or manually adjusting natural frequencies can widen the energy capture band. The most commonly used method in frequency tuning is to regulate the stiffness or mass of the system. Chen et al. (Lihua et al. 2020) designed a PEH device with adjustable centroid containing rolling balls is proposed. This PEH can collect power in the frequency band from 16 to 25 Hz. Shi et al. (2020) proposed a broadband PEH with active self-tuning frequency. By changing the position of the T-shaped section, it can adjust the resonance frequency of the PEH to match the external excitation. Static deflection and overall volume will increase due to changes in stiffness and mass of the system. The scheme is complicated in design and superior in the mechanical loss.

Multiple degree-of-freedom (DOF) energy harvesting is one strategy for achieving broadband goals (Aramaki et al. 2019; Thein et al. 2019; Suresh et al. 2019) developed a 2-DOF system with a dynamic magnifier. The elastic amplifier combines a four-bar mechanism and a helical spring. Lan et al. (2019) investigated the galloping based PEH, and analyse the potential advantages of the 2-DOF galloping based PEH over the conventional single DOF galloping based PEH. A six-DOF PEH with linear and rotational vibration based on parallel mechanism is proposed by Yuan et al. (Yuan and Wang 2017)

Nonlinear piezoelectric vibration energy harvesting technology is a different strategy for broadband energy capture. Compared with linear PEH, nonlinear PEH has the characteristics of a wide frequency band and higher power generation efficiency. There are two main ways to introduce nonlinear stiffness: nonlinear magnetic force (Shan et al. 2018; He et al. 2020) and piecewise linear structure (Staaft et al. 2018; Xie et al. 2019). The nonlinearity caused by the magnetic force also plays an important role in widening the frequency band and improving energy-trapping efficiency. Shu et al. (2018) proposed an energy harvesting device based on non-contact rotating magnetic attraction. Due to frequency up-conversion, it exhibits a broadband frequency response. Zhao et al. (2019a, b) proposed a research method using magnetic couple and bending amplification mechanism to improve the robustness of the entire system. Na et al. (2020) proposed a new type of wind energy harvester device through magnetic coupling based on rotating structure. The deflection and output power of the piezoelectric beams gradually increase with the increase of wind speed.

The organic combination of multiple broadband measures is a new method to achieve broadband energy harvesting, it can harvest energy more effectively in a wider working frequency domain by reasonably using a variety of broadband

methods to overcome the defects of a single broadband mechanism (Xiong et al. 2016; Sun and Tse 2019). A kind of magnetocouple PEH based on parasitic vibrator structure is proposed by Wang and Tang (2017). The parasitic vibrator can produce two resonance peaks, thereby achieving broadband electrical output. Nguyen et al. (2019) presented the magnetically coupled 2-DOF energy harvester with secondary intrawell resonances. Higher electrical power is generated and the operating frequency bandwidth is increased. Xie et al. (Zhao et al. 2019a, b) designed a T-shaped magnetically coupled PEH with multiple resonance frequencies. Under low-frequency excitation, it can achieve an ultra-wide working frequency range. Wang et al. (2021) listed in detail the current status of development of various types of rotary harvesters and compared them.

This paper proposes a magnetically excited rotating piezoelectric energy harvester (MER-PEH) to effectively collect energy and expand working bandwidth. The nonlinear electromechanical model of MER-PEH is established. The effect of different vibrator configurations on the resonant peaks of the MER-PEH is investigated theoretically and experimentally. A prototype of a collector and energy harvester circuit was manufactured and tested, which converts the generated alternating current (AC) power into ordered current (DC) power and lights up the LED lights. The effect of load resistance on the nonlinear response and power output is also investigated. This result clearly shows that it has good harvester performance under low-frequency excitation to power tiny wireless sensing devices.

2 Design and modelling

2.1 The working principle

Figure 1 shows the proposed MER-PEH model design with four piezoelectric beams (A1, A2, B1, and B2), four magnets, a rotamer, a support plate, a slip ring. The support plate is fixed on the optical platform by bolts. The piezoelectric beams (A1 and A2) and piezoelectric beams (B1 and B2) are fixed on the rotamer and support plate by screw bolts, respectively. The angles of piezoelectric beams A and B installed on the rotamer and support plate are 60 and 90 degrees, respectively. The piezoelectric beams are made of PZT and copper plates glued together. Magnets of different masses are adhered to the free end of the piezoelectric beams to coordinate the natural frequency. The material of the magnet is a NdFeB. The support plate, and the rotamer are made by A3S 3D printer (JGAURORA) using PLA material. The parameters of the prototype are shown in Table 1. The prototype shown in Fig. 1 can be considered as

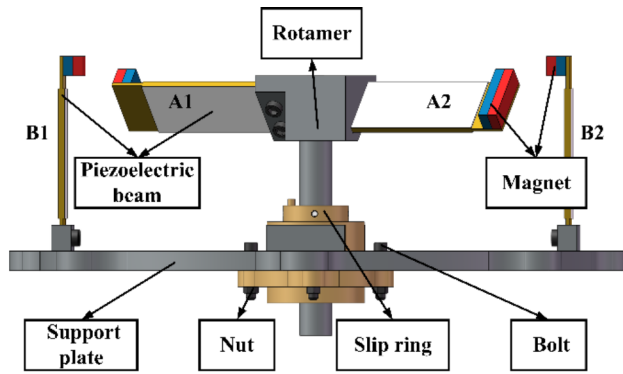


Fig. 1 Photograph of the prototype energy harvester

Table 1 Parameters of a prototype MER-PEH

Parameter	Value
PZT	
Length l_p	0.04 m
Width b_p	0.02 m
Thickness h_p	0.0002 m
Density ρ_p	7700 kg/m ³
Young's modulus E_p	70 GPa
Coupling coefficient d_{31}	-285*10 ⁻¹² C/N
Laminate permittivity ϵ_r	3200 ϵ_0
Permittivity of free space ϵ_0	8.854*10 ⁻¹² F/m
Copper plate	
Length l_s	0.06 m
Width b_s	0.02 m
Thickness h_s	0.0003 m
Density ρ_s	7800 kg/m ³
Young's modulus E_s	200 GPa
Magnet	
Magnet A/B/C	5 g/6 g/7 g
Magnet's residual flux density B_r	1.2T

a cylinder with a diameter of 0.15 m and a height of 0.03 m, with a total mass of about 0.2 kg.

The rotation of the rotamer drives piezoelectric beams (A1 and A2) to rotate. During the rotation, the interaction of magnets at the free ends drives the piezoelectric beams (B1 and B2) to swing left and right. Piezoelectric beam A is deformed by rotating centrifugal force and magnetic force, and piezoelectric beam B is deformed by magnetic force. The piezoelectric beams vibrate at its natural frequency and convert vibration energy into electrical energy due to the piezoelectric effect. The harvester can be applied to devices with rotary motion such as wheels and fans.

2.2 Modelling analysis

The electromechanical coupling model of the piezoelectric system is developed on the basis of the Hamiltonian

principle. The kinetic energy of the piezoelectric system can be expressed as:

$$T = \int_0^{l_s} m_{bs}\dot{w}_1^2 dx + \int_0^{l_s} m_{bs}\dot{w}_2^2 dy + 2 \int_0^{l_p} m_{bp}\dot{w}_1^2 dx + 2 \int_0^{l_p} m_{bp}\dot{w}_2^2 dy + m_1\dot{w}_1^2 + m_1\dot{w}_2^2 \tag{1}$$

where m_b is the masses per unit length of the rectangular piezoelectric beam; m_l is the mass of the rectangular magnet mass; l is the length of the rectangular piezoelectric beam; w_1 and w_2 is the longitudinal motions of the subsystem piezoelectric beam A and B masses, respectively. The piezoelectric beam is made of PZT and copper plates glued together. Two piezoelectric elements are surface bonded on both sides of the copper substrate by an enhanced coupling approach with edge elements. The subscript s is the copper substrate, and the subscript p is the piezoelectric element.

The potential energy of the entire structural system can be written as:

$$U = \int_0^{l_s} EI \left(\frac{\partial^2 w_1}{\partial x^2} \right)^2 dx + \int_0^{l_p} EI \left(\frac{\partial^2 w_2}{\partial y^2} \right)^2 dy - 2J_p \left(V_1 \int_0^{l_s} \frac{\partial^2 w_1}{\partial x^2} dx + V_2 \int_0^{l_p} \frac{\partial^2 w_2}{\partial y^2} dy \right) - C_{p1} V_1^2 - C_{p2} V_2^2 + 2 \int_0^{l_s} m_b g w_1 dx + 2 \int_0^{l_p} m_b g w_2 dx + 2m_1 g w_1 + 2m_1 g w_2 + 4 \int_0^y F_m dy + k(w_1 + w_2) \tag{2}$$

where V_1 and V_2 are the voltages respectively generated by the subsystems piezoelectric beam A and piezoelectric beam B; C_{p1} and C_{p2} are the clamped capacitance of the subsystems piezoelectric beam A and B piezoelectric patch element, respectively; k is the effective stiffness; EI is the stiffness of the rectangular piezoelectric beam; J_p is the electromechanical coupling term; g is the gravitational acceleration. F_m is the normal magnetic force between the two rectangular permanent magnets Fig. 2.

The normal force F_m can be written as (Zhao et al. 2019a, b):

$$F_m = F_{mag} |\sin(vn\pi t)| \tag{3}$$

where t is time; v is the rotational speed of the revolving host; n is the number of a driving magnet; F_{mag} is the repulsive magnetic force between rectangular permanent magnets.

The repulsion magnetic force between two rectangular permanent magnets is expressed as (Wang et al. 2021):

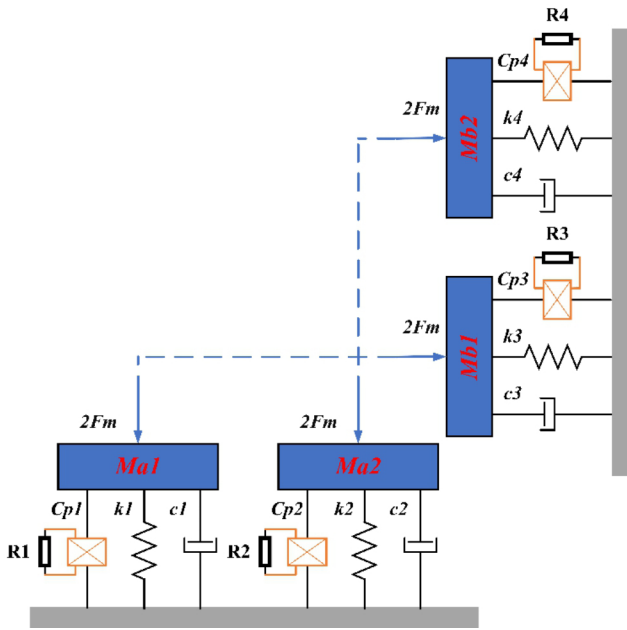


Fig. 2 Piezoelectric vibration energy harvesting system model

$$F_{mag} = \frac{2}{1(1+3Z)} \times \frac{W_m H_m}{2\mu_k} \times \frac{B_r^2}{\pi^2} \times \left(\begin{matrix} \tan^{-1} \frac{W_m H_m}{2Z\sqrt{W_m^2 + H_m^2 + 4Z^2}} \\ -\tan^{-1} \frac{W_m H_m}{2(L_m + Z)\sqrt{W_m^2 + H_m^2 + 4(L_m + Z)^2}} \end{matrix} \right)^2 \quad (4)$$

where L_m represents the length of the rectangular magnet; W_m represents the width of the rectangular magnet; H_m represents the height of the rectangular magnet; μ_k denotes the permeability of the rectangular magnet; B_r represents the magnetic flux density on the polar surface of the magnet; Z represents the distance between two rectangular magnets.

The Lagrangian function expression of the system can be described as:

$$L = T - U \quad (5)$$

The virtual work of piezoelectric system can be expressed as:

$$\delta W = - \sum_{i=1}^4 \int_0^L c_i \dot{w}_i \delta w_i dx_i + Q_i \delta V_i \quad (6)$$

where c is the equivalent damping coefficient of the subsystem; δ is the contradistinction operator; Q is the charge of the piezoelectric element.

The average stresses on the surface of the piezoelectric beam can be calculated as:

$$\sigma = \frac{lh_e k_s X}{[(bh_p^3/3) + 4bh_p h_e^2] + E_s b h_s^2 / 6E_p} \quad (7)$$

$$h_e = \frac{(2h_p + h_s)}{2} \quad (8)$$

where X is the maximum displacement amplitude of the mass; b and h are the width and thickness of the piezoelectric beams, respectively; h_e is the equivalent thickness of the Piezoelectric beam. The relationship between output voltage and time t can be expressed as:

$$V_o = \frac{-d_{31} h_p \sigma}{2\epsilon_r \epsilon_0} e^{-(c/2\sqrt{km})\omega t} \sin \omega_d t \quad (9)$$

where d_{31} is the piezoelectric strain constant, ϵ_r is the dielectric constant of the piezo material, ϵ_0 is the permittivity of free space, ω_d and ω are the damped natural frequency and the resonant frequency of the spring-mass system, respectively.

The output power of the MER-PEH can be calculated from the voltage value across the load:

$$P = \frac{V^2}{R} \quad (10)$$

Based on the extended Hamilton principle, Lagrangian electromechanical equations are:

$$\begin{cases} \frac{d}{dt} \left(\frac{\partial L}{\partial \dot{w}_i} \right) - \frac{\partial L}{\partial w_i} = \frac{\delta W}{\delta \dot{w}_i} \\ \frac{d}{dt} \left(\frac{\partial L}{\partial \dot{v}_i} \right) - \frac{\partial L}{\partial v_i} = \frac{\delta W}{\delta \dot{v}_i} \end{cases} \quad (11)$$

Therefore, the dynamic model of electromechanical coupling can be derived from Eq. 11, which is specifically expressed as:

$$\begin{cases} M_i \ddot{w}_i + c_i \dot{w}_i + k_i w_i - \theta_i V_i + m_1 g + F_m = 0 \\ C_p \dot{V}_i + \frac{V_i}{R_L} + \theta_i \dot{w}_i = 0 \end{cases} \quad (12)$$

where M is the equivalent mass of the subsystem; θ is the equivalent electromechanical coupling coefficient; k is the effective stiffness of the nonlinear configuration; R_l is the equivalent resistance which is matched with piezoelectric beams.

3 Experiments and results

A series of experiments are tested to verify the theoretical model and performance of MER-PEH. Figure 3 describes the entire test system including a controller, a stepper motor, a piezoelectric energy harvester prototype, a resistance box, and a digital oscilloscope. Stepper motor is used as power source. The controller is used to control the rotational speed of the stepper motor. And the rotamer is driven by a stepper motor. The piezoelectric cantilever beams vibration generates electrical energy under the excitation of the magnet. The output voltage of the MER-PEH is measured by a digital oscilloscope (DS4043 RIGOL). In order to measure the resistance characteristics of the MER-PEH and seek the best power under different resistance, the measurement was carried out by using a resistance box (ZX21e FUYANG). Figure 4 describes a rectifier bridge is used as a rectifier device to convert AC to DC which can directly light up the LEDs.

According to the equation derived above, it is clear that the output performance of the harvester is related to the magnitude of the excitation, as well as its own natural frequency. When the excitation frequency is close to the natural frequency of the harvester, the greater the excitation, the greater the deformation of the piezoelectric vibrator and the greater the output voltage of the harvester. The excitation

is adjusted by changing the mass of the magnets and the distance between the magnets on piezoelectric beam A and piezoelectric beam B.

To adjust the natural frequency of the MER-PEH, the influence of different weights of cutting-edge mass magnets on power generation performance was tested. In the case where the radial excitation interval is 10 mm, the experiment tested a device that only contains two piezoelectric elements A1 and B1. Figure 5 (a) and (b) display the influence of the mass of the magnet on piezoelectric power generation. It shows that the mass of the magnet fixed on the free end of the piezoelectric beams is 5 and 6 g, it has the lowest and largest open-circuit voltage, respectively. As shown in Fig. 5(a), the output voltage at the peak point of the prototype is maximum when the magnet mass is 6 g. Figure 5(b) shows that the peak store voltage is not only larger at a magnet mass of 6 g, but the output voltage at high speed is still more than 5 V. Therefore, the best output performance of the prototype is achieved when the magnet mass is 6 g. At different rotation speeds of 250, 600, and 800 r/min, the A1 piezoelectric beam has three different peak voltage respectively. And the B1 piezoelectric beam has three peak voltages at the rotation speed of 200 r/min, 400 r/min, and 650 r/min. A1 and B1 piezoelectric beams have three voltage extreme points respectively, which are 20.56 V, 20.94 V, 19.06 V, and 16.56 V, 18.12 V, 9.68 V.

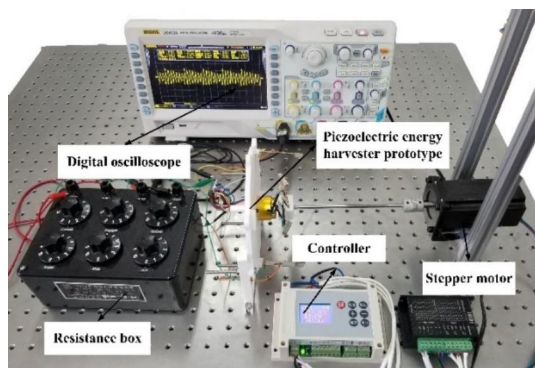


Fig. 3 Experimental setup of the PEHS

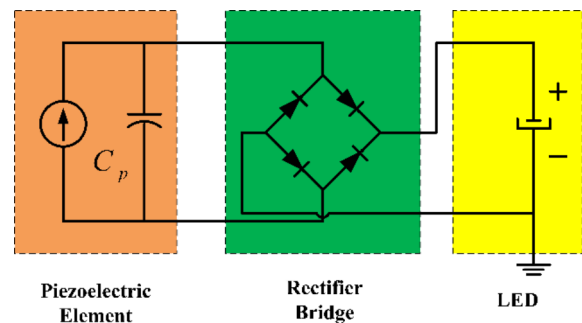


Fig. 4 The circuit schematic diagram of the system

Fig. 5 The open-circuit voltage vs. rotational speed with different magnetic mass: (a) the piezoelectric beam A1, (b) the piezoelectric beam B1

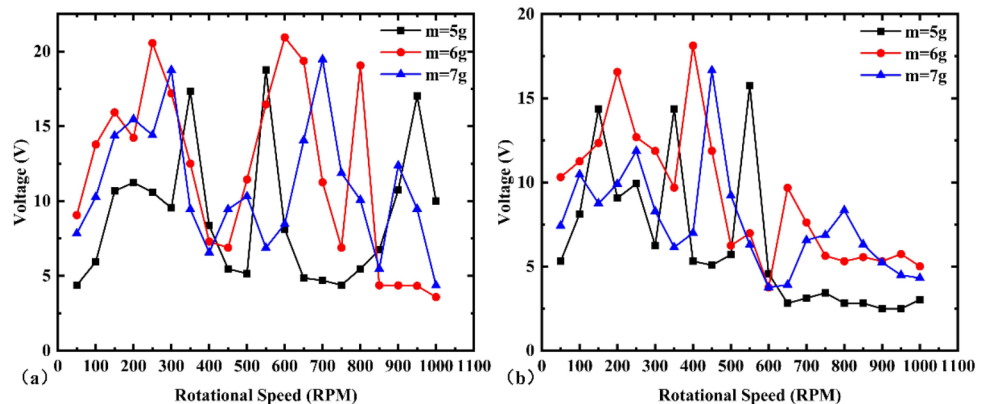


Figure 6 (a) and (b) show the effect of the distance between two magnets on power generation performance. In the case where the magnet mass is 6 g, the experiment tested a device that only contains two piezoelectric beams A1 and B1. The output voltage of the piezoelectric beams is the largest at this time when the radial spacing between the two magnets is 5 mm. It shows the difference magnetic force caused by different spacings will affect the output voltage of the piezoelectric beams. The peak voltage will increase as the distance between the magnets decreases under the action of repulsive force. It also demonstrates that the radial distance between the two magnets will affect the magnetic force and the magnetic force increases as the distance between the magnets decreases. However, the distance between the two magnets cannot be reduced infinitely because of the physical properties of the piezoelectric beam. If the distance between the two magnets is too small causing an excessive magnetic force, the piezoelectric beams itself will be damaged. Therefore, the minimum radial excitation interval in the experimental research is 5 mm. The A1 piezoelectric beam has four voltage peaks at the rotation speed of 150 r/min, 300 r/min, 400 r/min, and 700 r/min, and the B1 piezoelectric beam has three peak voltages at the rotation speed of 300 r/min, 500 r/min, and 750 r/min. The four output voltage of the A1 piezoelectric beam are 27.5 V,

26.31 V, 25.93 V, and 24.68 V. The three voltage of the B1 piezoelectric beam are 22.51 V, 21.87 V, and 22.99 V.

At the same time, the different connection methods between the vibrators of MER-PEH has studied. Figure 7 (a) and (b) describe the relationship between rotational speed and voltage in different connection modes. When the radial excitation interval is 5 mm and the mass of the magnet is 6 g, an experimental test is performed. The symbol for the circuit series connection is +, // represents the circuit parallel connection. The A piezoelectric beam has three voltage peaks at the rotation speed of 150 r/min, 250 r/min, and 550 r/min. The B piezoelectric beam has three peak voltages at the rotation speed of 300 r/min, 550 r/min, and 800 r/min. A and B piezoelectric beams have three voltage extreme points respectively, which are 31.25 V, 42.39 V, 43.24 V and 34.13 V, 34.69 V, 17.51 V. Compared with the other two connection methods, the piezoelectric beams A and B have the largest open-circuit voltage when the vibrator is connected in series.

Figure 8 describes the correlation curve between output voltage of MER-PEH and rotational speed in different connection modes. It can be seen that there are multiple piezoelectric vibrators in the energy harvesting system, and the connection mode of each piezoelectric vibrator is series, the power generation effect is the best. The MER-PEH system has three higher peak points when the rotation speed is

Fig. 6 The output voltage vs. rotational speed at different radial excitation intervals: (a) the piezoelectric beam A1, (b) the piezoelectric beam B1

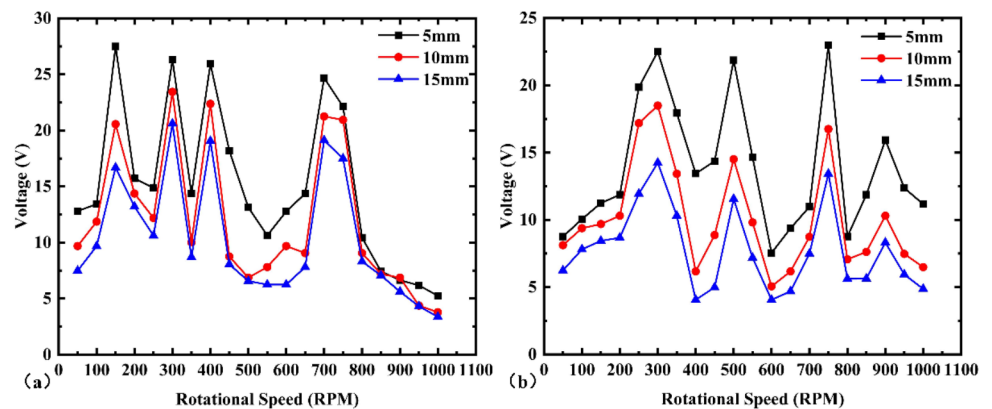
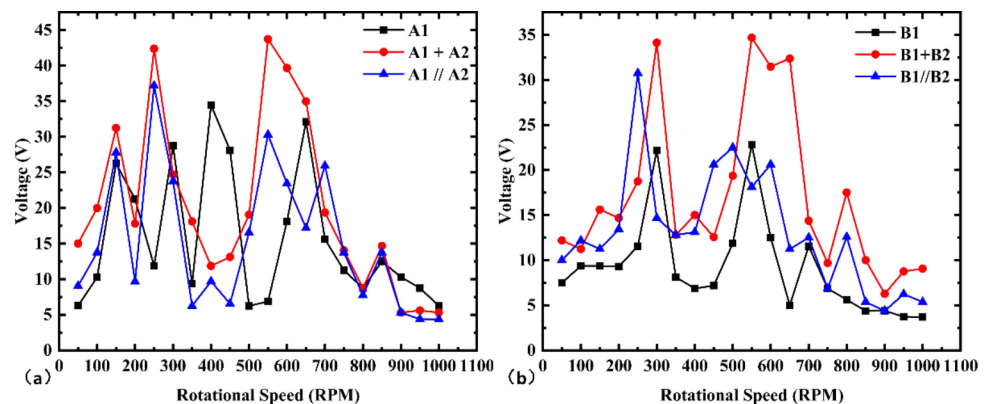


Fig. 7 The output voltage vs. rotational speed at different circuit connection methods: (a) the piezoelectric elements A, (b) the piezoelectric elements B



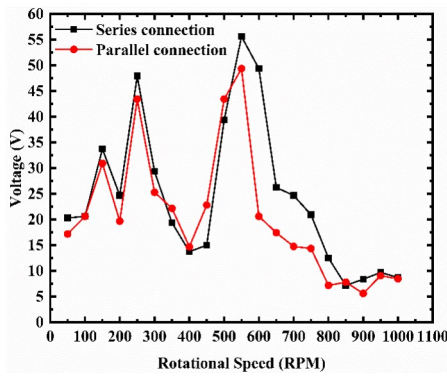


Fig. 8 The output voltage of MER-PEH vs. rotational speed at different circuit connection methods

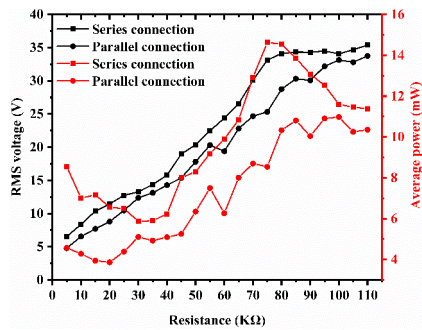


Fig. 9 Resistance vs. the average power and the RMS voltage at different circuit connection methods

150 r/min, 250 r/min, and 550 r/min. The output voltages obtained are 33.76 V, 47.93 and 55.62 V. Compared with the other two connection methods, MER-PEH has the largest open-circuit voltage when the vibrator is connected in series. Within a certain range of rotational speed, multiple peak points can be taken, so the working bandwidth of the piezoelectric beam is increased to a certain extent.

Figure 9 describes the correlation curve between output voltage and power under different circuit connection modes and different resistance. The experiment is tested when the rotation speed is 550 r/min, the mass of the magnet is 6 g, the radial excitation distance is 5 mm. Experimental results show that the voltage of the load resistor also increases as the resistance of the load resistor increases. The maximum voltages of the series circuit and the parallel circuit are 46.43 V and 20.84 V, respectively. As the load resistance increases, the average power output of MER-PEH will first increase and then decrease and the performance in series is better than in parallel. So, when the average output power is 14.625 mW and the load is 75 kΩ, the energy harvesting system can light up 260 LED lights in parallel under the action of the rectifier bridge.

4 Summary

In this paper, a MER-PEH applied in rotational motion is proposed, the parametric variables related to the output of MER-PEH, including the mass of the magnet, the distance between the magnet on piezoelectric beam A and piezoelectric beam B, and the way the piezoelectric vibrator is connected, are first analyzed theoretically. Then an experimental system was fabricated and built for verification. The experimental results showed that the quality of the magnet, the distance of the magnet and the connection of the piezoelectric vibrator played a decisive role in the output performance of the prototype. The magnet mass is 6 g and the distance is 5 mm as the optimal variables, at which time the prototype has more than 15 V output at 0–11 Hz rotation frequency, and the maximum voltage reaches 34.69 V. Also by connecting the piezoelectric vibrator in series, the maximum output voltage of the prototype is increased by 152%. Under this condition, the maximum output power of the prototype reaches 14.625 mW when the speed is 550 r/min. The final prototype powers small electronic devices at maximum output power and the prototype can light up to 260 LEDs, which proves the possibility of the prototype as a power source for wireless electronic devices. In short, it is a new way to broaden the bandwidth of piezoelectric energy harvesters as well as to wirelessly power small electronic devices.

Acknowledgements This work was supported by the NSFC of China (No. 51805489), the National Study Abroad Fund of China (No. 202008220173) and Project of Jilin Provincial Education Department: Research on River Hydrological Monitoring Device Based on ADCP Sensor under Grant jijiaoheze [2014] no. 140.

References

Aramaki M, Yoshimura T, Murakami S, Kanda K, Fujimura N (2019) Electromechanical characteristics of piezoelectric vibration energy harvester with 2-degree-of-freedom system. *Appl Phys Lett* 114:13

Binyet E, Huang C-Y, Chang J-Y (2018) Characterization of a vortex-induced vibrating thin plate energy harvester with particle image velocimetry. *Microsyst Technol* 24(11):4569–4576

Deng L, Fang Y, Wang D, Wen Z (2018) A MEMS based piezoelectric vibration energy harvester for fault monitoring system. *Microsyst Technol* 24(9):3637–3644

Halim MA, Park JY (2017) Piezoelectric energy harvester using impact-driven flexible side-walls for human-limb motion. *Microsyst Technol* 24(5):2099–2107

He L, Wang Z, Wu X, Zhang Z, Zhao D, Tian X (2020) “Analysis and experiment of magnetic excitation cantilever-type piezoelectric energy harvesters for rotational motion,” *Smart Materials and Structures*, vol. 29, no. 5,

Kamenar E et al (2015) “Harvesting of river flow energy for wireless sensor network technology,”. *Microsyst Technol* 22(7):1557–1574

- Lan C, Tang L, Hu G, Qin W (2019) “Dynamics and performance of a two degree-of-freedom galloping-based piezoelectric energy harvester,” *Smart Mater. Struct.*, vol. 28, no. 4,
- Li P, Gao S, Zhou X, Liu H, Shi J (2017) Analytical modeling, simulation and experimental study for nonlinear hybrid piezoelectric–electromagnetic energy harvesting from stochastic excitation., *Microsyst Technol* 23(12):5281–5292
- Lihua C, Jiangtao X, Shiqing P, Liqi C (2020) “Study on cantilever piezoelectric energy harvester with tunable function,” *Smart Mater. Struct.*, vol. 29, no. 7,
- Makki N, Pop-Iliev R (2012) Battery-and wire-less tire pressure measurement systems (TPMS) sensor., *Microsyst Technol* 18:7–8
- Mangaiyarkarasi P, Lakshmi P, Sasrika V (2019) Enhancement of vibration based piezoelectric energy harvester using hybrid optimization techniques., *Microsyst Technol* 25(10):3791–3800
- Na Y, Lee M-S, Lee JW, Jeong YH (2020) “Wind energy harvesting from a magnetically coupled piezoelectric bimorph cantilever array based on a dynamic magneto-piezo-elastic structure,” *Applied Energy*, vol. 264,
- Nguyen MS, Yoon Y-J, Kim P (2019) Enhanced Broadband Performance of Magnetically Coupled 2-DOF Bistable Energy Harvester with Secondary Intrawell Resonances., *Int J Precision Eng Manufacturing-Green Technol* 6(3):521–530
- Shan G, Wang DF, Song J, Fu Y, Yang X (2018) A spring-assisted adaptive bistable energy harvester for high output in low-excitation. *Microsyst Technol* 24(9):3579–3588
- Shi G, Yang Y, Chen J, Peng Y, Xia H, Xia Y (2020) “A broadband piezoelectric energy harvester with movable mass for frequency active self-tuning,” *Smart Mater. Struct.*, vol. 29, no. 5,
- Shu YC, Wang WC, Chang YP (2018) “Electrically rectified piezoelectric energy harvesting induced by rotary magnetic plucking,” *Smart Mater. Struct.*, vol. 27, no. 12,
- Somkuwar R, Chandwani J, Deshmukh R (2018) Wideband auto-tunable vibration energy harvester using change in centre of gravity. *Microsyst Technol* 24(7):3033–3044
- Staafl LGH, Smith AD, Köhler E, Lundgren P, Folkow PD, Enoksson P (2018) Achieving increased bandwidth for 4 degree of freedom self-tuning energy harvester., *J Sound Vibrat* 420:165–173
- Sun S, Tse PW (2019) Modeling of a horizontal asymmetric U-shaped vibration-based piezoelectric energy harvester (U-VPEH),. *Mech Syst Signal Process* 114:467–485
- Suresh K, Shankar K, Sujatha C (2019) “A novel passive mechanism to improve power output in 2DOF piezoelectric vibration energy harvester,” *Smart Mater. Struct.*, vol. 28, no. 11,
- Thein CK, Foong FM, Shu Y-C (2019) Spring amplification and dynamic friction modelling of a 2DOF/2SDOF system in an electromagnetic vibration energy harvester – Experiment, simulation, and analytical analysis., *Mech Syst Signal Process* 132:232–252
- Wang H, Tang L (2017) Modeling and experiment of bistable two-degree-of-freedom energy harvester with magnetic coupling., *Mech Syst Signal Process* 86:29–39
- Wang Z et al (2021) “Rotational energy harvesting systems using piezoelectric materials: A review,” (in English), *Rev. Sci. Instrum.*, Review vol. 92, no. 4, p. 19, Apr Art no. 041501
- Xie Z, Wang T, Kwuimy CAK, Shao Y, Huang W (2019) Design, analysis and experimental study of a T-shaped piezoelectric energy harvester with internal resonance., *Smart Mater Struct* 28:8
- Xiong L, Tang L, Mace BR (2016) “Internal resonance with commensurability induced by an auxiliary oscillator for broadband energy harvesting,” *Applied Physics Letters*, vol. 108, no. 20,
- Yuan G, Wang DH (2017) “A piezoelectric six-DOF vibration energy harvester based on parallel mechanism: dynamic modeling, simulation, and experiment,” *Smart Mater. Struct.*, vol. 26, no. 3,
- Zhao L-C et al (2019a) “Magnetic coupling and flextensional amplification mechanisms for high-robustness ambient wind energy harvesting,” *Energy Convers. Manage.*, vol. 201,
- Zhao Z, Wang T, Zhang B, Shi J (2019b) “Energy Harvesting from Vehicle Suspension System by Piezoelectric Harvester,” *Mathematical Problems in Engineering*, vol. pp. 1–10, 2019b

Publisher’s note Springer Nature remains neutral with regard to jurisdictional claims in published maps and institutional affiliations.